Applied Element Modelling of the Out-of-Plane Bending Behaviour of Single Leaf Unreinforced Masonry Walls

Nouman Khattak[1], Hossein Derakhshan[2], David P Thambiratnam[3] and Nimal Jayantha Perera[4]

1. PhD Student, School of Civil and Environmental Engineering, Queensland University of Technology, 2 George St, Brisbane City QLD 4000, Australia, nouman.khattak@hdr.qut.edu.au

2. Lecturer, School of Civil and Environmental Engineering, Queensland University of Technology, 2 George St, Brisbane City QLD 4000, Australia, hossein.derakhshan@qut.edu.au

3. Professor, School of Civil and Environmental Engineering, Queensland University of Technology, 2 George St, Brisbane City QLD 4000, Australia, d.thambiratnam@qut.edu.au

4. Principal Consultant, Kasina Consultants Pty Ltd, QLD, Australia, njp@kasinaconsultants.com

Abstract

Masonry is a composite material consisted of units and mortar that have a non-linear behaviour. Therefore, its numerical modelling presents several challenges. Different modelling techniques are available for masonry material including Applied Element Method (AEM). This research was aimed at validating AEM numerical models against existing experimental data. The data represents typical Australian single-leaf unreinforced masonry walls loaded in the out-of-plane (OOP) direction. A total of eight tested walls from the related literature were analysed to study the modelling technique. The walls had different geometry, openings and overburden loads. Although the test data has previously been validated using different numerical tools, the employed AEM assisted in a more accurate prediction of the behaviour and crack patterns. From this study, it was concluded that AEM not only predicted the experimental results with good accuracy but it also predicted a realistic crack patterns that matched experimentally observed damages.

Keywords: masonry; out-of-plane; numerical modelling; applied element method (AEM).

1 Introduction

Masonry is a composite/non-homogeneous and anisotropic material, being comprised of units and mortar. The combined mechanical behaviour of masonry composite is non-linear. Due to this compositeness and non-linearity, masonry analysis is considered as a sophisticated problem. There are many techniques/methods and numerical tools to numerically model unreinforced masonry as explained by D'Altri et al. (2019). In the related literature, three major modelling methods are commonly applied namely micro, simplified micro or meso, and macro-modelling (Asteris et al. 2015).

Amongst the numerical methods, applied element method (AEM) is a numerical modelling strategy that was first introduced in the 1990s by Meguro and Tagel-Din (1997). It is an

alternative simulation technique to the finite element method (FEM), with the main difference being that the elements in the FEM are connected by nodes whereas in AEM they are connected by a set of springs (including normal and shear springs) without nodal connectivity. This way of elements connectivity provides an extra edge to AEM as it can predict not only the initial cracking, peak behaviour and post-peak behaviour but also the separation of the elements that reach their maximum capacities (Meguro and Tagel-Din 1997). The springs are responsible for transferring load and modeling deformations between elements, while elements in AEM carries only mass and damping of the system (Malomo et al. 2018a, 2018b). Degrees of freedom in AEM are assigned to the centroid of rigid elements thus resulting in 6 degrees of freedom (three translational and three rotational), whereas in FEM degrees of freedom are assigned to the nodes, meaning 24 degrees of freedom per element. These capabilities of AEM makes a direct representation of the real-world behaviour of any structure possible with reduced simulation run time compared to FEM (Grunwald et al. 2018).

AEM has been successfully applied to predict the response of URM walls including both the in-plane and out-of-plane behaviour (Malomo et al. 2018a, 2018b). For in-plane response, four slender walls and two squat walls that had been subjected to cyclic loading in-plane loading were selected (Malomo et al. 2018a). Out of the four slender walls, three were made of clay and one of calcium-silicate bricks. Of squat walls, one was made of clay bricks and the other of calcium-silicate bricks. For OOP response, four walls were validated, one being single-leaf and three being cavity walls subjected to shake table tests. The three cavity walls were made of a combination of clay and calcium-silicate bricks, with having calcium-silicate brick as inner wall and clay brick as outer wall with different vertical load. Malomo et al. (2020a) predicted the dynamic response of full-scale clay brick masonry buildings with flexible diaphragm. Malomo et al. (2021) validated the shake table test conducted on typical URM cavity wall building prevalent in Groningen region, Netherlands with openings and flexible diaphragm. In another study by Malomo et al. (2020b, 2020c), more experimental campaigns performed on URM buildings with flexible diaphragms were validated. Recently, Calò et al. (2021) simulated the dynamic response of a shake-table-tested full-scale URM building specimen having flexible timber diaphragms, a tall gable and two chimneys.

In this study, eight walls (S1-S8) that were tested under static out-of-plane pressure load by Griffith and Vaculik (2007) are modelled using AEM and numerical outcomes are compared with experimental results. In order to carry out the modelling, a structural analysis software tool called Extreme Loading for Structures (ELS) version-8, developed by ASI (2020), was employed. This experimental program, chosen for validation, has already been successfully validated previously using different numerical techniques including finite element method (FEM), Discrete Element method (DEM) and Applied Element Method (AEM). Noor-E-Khuda et al (2016), Jough & Golhashem (2020) and Yu et al. (2008) validated several walls using FEM. Gálvez et al. (2017) employed DEM and successfully validated pressure-displacement behaviour and cracks patterns of these walls. In another study, Gálvez et al. (2018) compared FEM and DEM for these walls. Adhikari and D'Ayala (2019) successfully validated wall S1 using AEM.

2 Experimental Details

Different configurations of URM walls were considered and tested under out-of-plane load by Griffith and Vaculik (2007). The specimens included solid walls, perforated walls with opening at one side, and short-spanned walls with opening at the middle. A total of eight walls were constructed, two walls were solid walls (S1 and S2) with and without axial compression load, four walls (S2 to S6) were having an opening 1200×946 mm^2 at one side of the wall and were subjected to varying axial load before OOP loading, two walls (S7 and S8) were short-spanned

walls (2520 mm) having an opening 1200×946 mm^2 at the middle with and without axial load. The height of all the walls were constant at 2494 mm. These walls were constructed using Australian standard face-perforated clay brick units of dimensions 230 × 110 × 76 mm (length × thickness × height) and bricks were laid in 10 mm thick weak mortar of the ratio 1:2:9 (cement:lime:sand) by volume. Each brick had 10 holes in two rows, five in each row. The density of the masonry was 1900 kg/mm^3. Two return walls of the length 480 mm were also constructed at both the ends. Sizes and details of these walls are given in Figure 1. Material properties are provided in Table 1. Normal text in the table represents material properties provided in literature (Vaculik 2012), whereas Italic text represents extra values required as input in the ELS software.

Different axial loads were considered for the wall specimens before applying OOP pressure. A 0.1 MPa load was applied for wall S1, S3 and S7. Half of it (0.05 MPa) was applied on wall S4. No axial load was applied to wall S2, S5, S6 and S8. The OOP pressure load was applied using air bags (Figure 2), while displacements at the middle of all walls, except wall S6 (where displacement was measured at the top mid-point) and wall S7 and S8 (where displacement was measured at the top of opening), were recorded using LVDTs. Displacement measurement locations are shown as small circles in Figure 1.

Same boundary conditions were employed for all the walls except wall S6 (In wall S6, the top edge of the wall was free without restrains). The return walls were restrained in such a way that the side edges can be treated as fixed supports. The bottom and top supports were simple supports thus allowing rotation. The boundary conditions are shown in Figure 1.

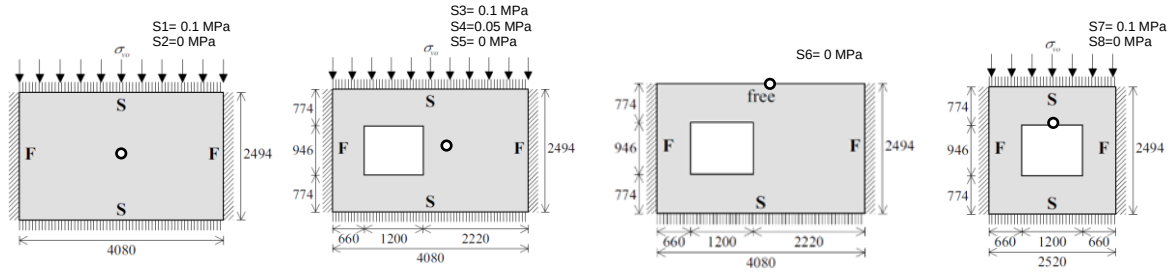

a) Wall S1 and S2 *b) Wall S3, S4 and S5* *c) Wall S6* *d) Wall S7 and S8*

Figure 1. Wall dimensions (in mm), boundary conditions (S means Simple support and F means Fixed support) and information about axial compression load given at top right corners (Vaculik 2012).

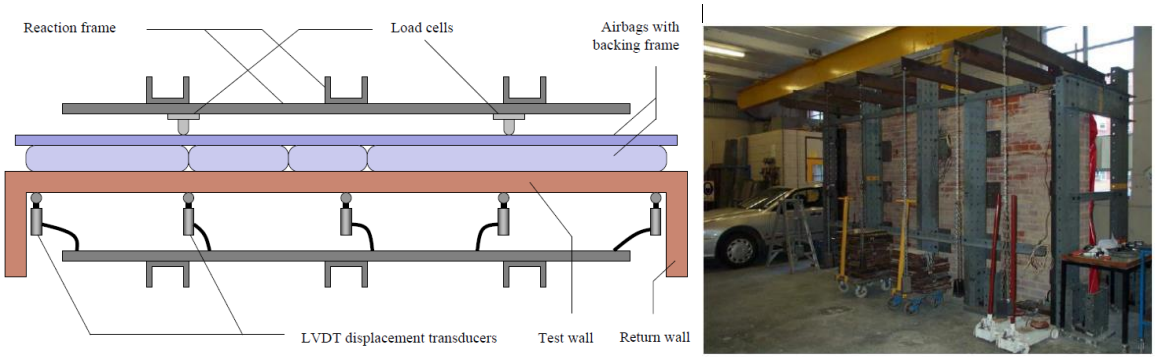

Figure 2. Experimental test setup (left) and arrangements for vertical loads (Right) (Vaculik 2012)

Table 1. Material Properties.

Wall ID	Brick						Mortar						Masonry				
	f_{bc}	E_b	G_b	f_{bt}	f_{bs}	f_{ut}	f_{jc}	E_j	f_{jt}	f_{js}	E_{av}	G_{av}	f_{mc}	E_m	G_m	f_{mt}	μ
S1	25	40300	16120	2.5	6.25	3.55	1.96	392	0.20	0.49	3139	1255	17.6	3190	1276	0.721	0.576
S2	25	61100	24440	2.5	6.25	3.55	1.35	271	0.14	0.34	2254	902	13.6	2240	896	0.520	0.576
S3	25	49000	19600	2.5	6.25	3.55	1.87	374	0.19	0.47	3040	1216	15.1	3030	1212	0.499	0.576
S4	25	37100	14840	2.5	6.25	3.55	3.61	722	0.36	0.90	5409	2163	16.8	5580	2232	0.635	0.576
S5	25	61400	24560	2.5	6.25	3.55	2.51	502	0.25	0.63	4064	1626	17.4	3990	1596	0.655	0.576
S6	25	52700	21080	2.5	6.25	3.55	1.67	335	0.17	0.42	2748	1099	15.8	2740	1096	0.496	0.576
S7	25	62000	24800	2.5	6.25	3.55	2.59	519	0.26	0.65	4196	1678	15.1	4130	1652	0.682	0.576
S8	25	63300	25320	2.5	6.25	3.55	1.87	375	0.19	0.47	3086	1234	16.1	3060	1224	0.714	0.576

Where: f_{bc}= average compressive strength of brick (MPa); E_b=modulus of elasticity of brick (MPa); G_b=shear modulus of brick (MPa), calculated as $E_b/2(1+v)$, v=0.25; f_{bt}=tensile strength of brick (MPa), assumed as 1/10th of compressive strength of brick; f_{bs}=shear strength of brick (MPa), assumed as 1/4th of compressive strength of brick; f_{ut}=average lateral modulus of rupture of brick (MPa); f_{jc}=compressive strength of mortar (MPa), assumed as E_j/200; f_{jt}=tensile strength of mortar (MPa), assumed as 1/10th of compressive strength of mortar; f_{js}=shear strength of mortar (MPa), assumed as 1/4th of compressive strength of mortar; E_{av}=average modulus of elasticity of masonry (MPa), calculated from equation 1; G_{av}=average shear modulus of masonry (MPa), calculated from equation 2; f_{mc}=compressive strength of masonry (MPa); E_m=modulus of elasticity of masonry (MPa); G_m=shear modulus of masonry (MPa), calculated as $E_m/2(1+v)$, v=0.25; f_{mt}=flexural tensile strength of masonry (MPa): μ = coefficient of friction.

3 Numerical Modelling

Applied element method is used to model the walls as shown in Figure 3. The numerical model was built in such a way to represent actual experimental conditions. In the numerical model, the whole brick was considered as a single element (although for more accuracy brick elements can further be divided into more elements), whereas mortar is represented by normal and shear springs (shear springs are in two directions). Therefore, the average properties of the brick-mortar combination were considered for the mortar springs. The mortar spring properties are calculated based on equation 1 and 2. Bricks are considered as solid element whereas mortar is represented by normal and shear springs (shear springs are in two directions).

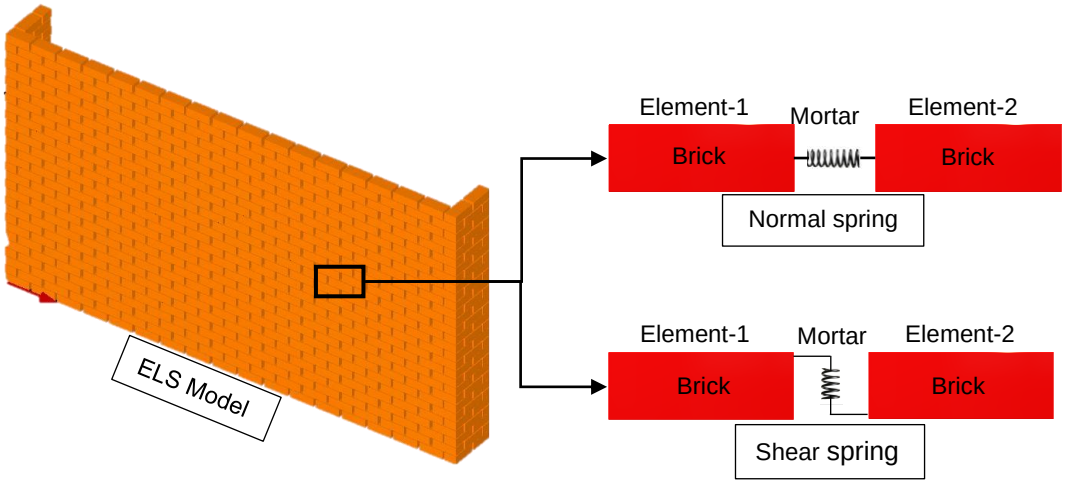

Figure 3. Numerical modelling of masonry using Applied Element Method (AEM).

The axial load was applied as line load (1.12 kg/mm for wall S1, S3 and S7 and 0.56 kg/mm for wall S4) over the top of the walls. The OOP load was applied as uniform pressure load at

the face of the wall. The resultant pressure shown in Figure 4 was calculated by adding the forces in each brick element in the OOP direction and diving by the area of the walls.

$$E_{av} = \frac{E_j \times E_b \times (t_j + t_b)}{E_j \times t_b + E_b \times t_j} \quad (1)$$

$$G_{av} = \frac{G_j \times G_b \times (t_j + t_b)}{G_j \times t_b + G_b \times t_j} \quad (2)$$

Where E_{av} is the average modulus of elasticity of the brick-mortar system (MPa) and G_{av} is the average shear modulus of the brick-mortar system (MPa). t_j is the thickness of mortar (mm) and t_b is the brick height (mm). For the mortar compressive strength, the compressive strength of masonry is used. This is because the mortar spring will be working in compression to transfer loads between bricks even after reaching the compressive strength

4 Results

The numerical results are compared with experimental results shown as plots in Figure 4. Within the plots, solid line represents the test observations, while a dashed line shows the results obtained from the numerical models. It is clearly shown that the numerical models developed has predicted the overall experimental behaviour well. The crack patterns produced during the numerical analysis matches well with the observed experimental cracks. However, for some walls a higher initial stiffness resulted from numerical models. It is important to mention that less than ten minutes were taken for each model to complete the simulation run using normal computer (Core i7 CPU @ 3.20GHz 3.19 GHz and 16GB RAM), which means saving in computational time.

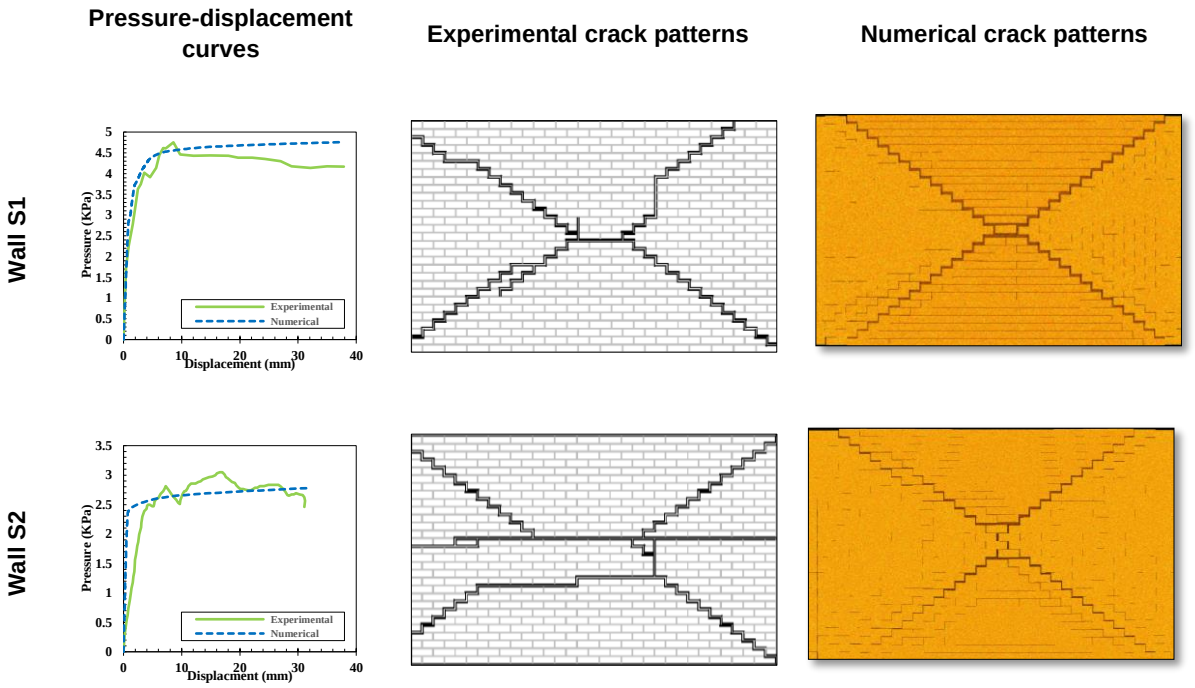

Wall S3

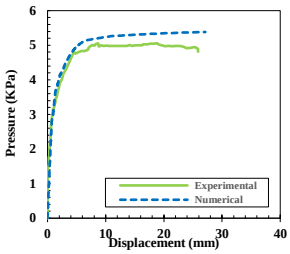

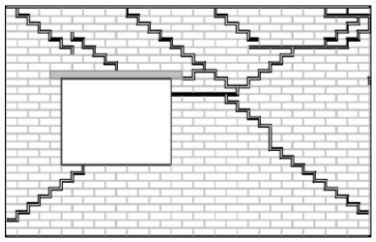

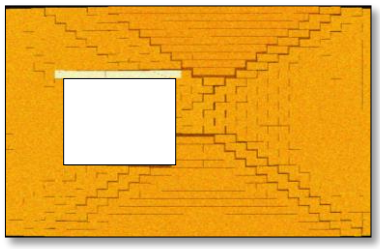

Wall S4

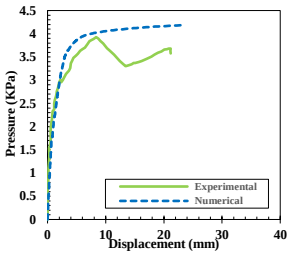

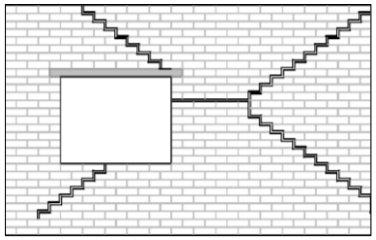

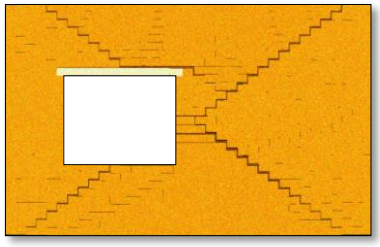

Wall S5

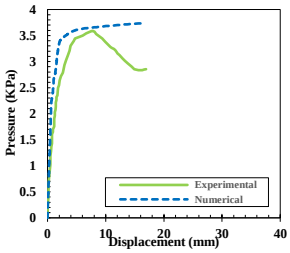

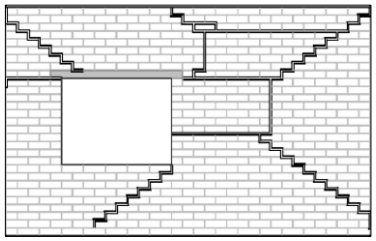

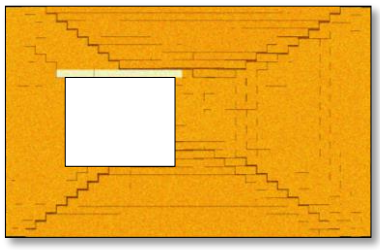

Wall S6

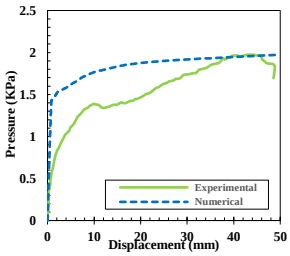

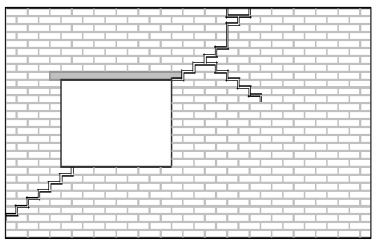

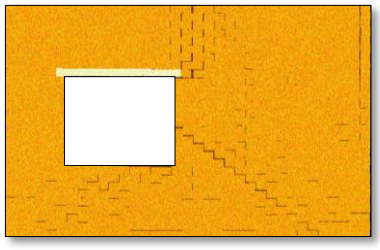

Wall S7

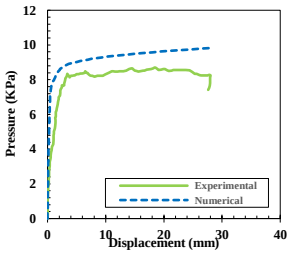

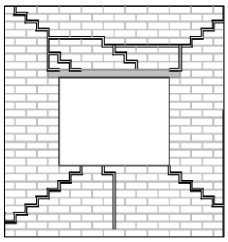

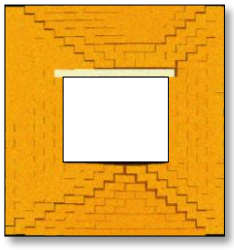

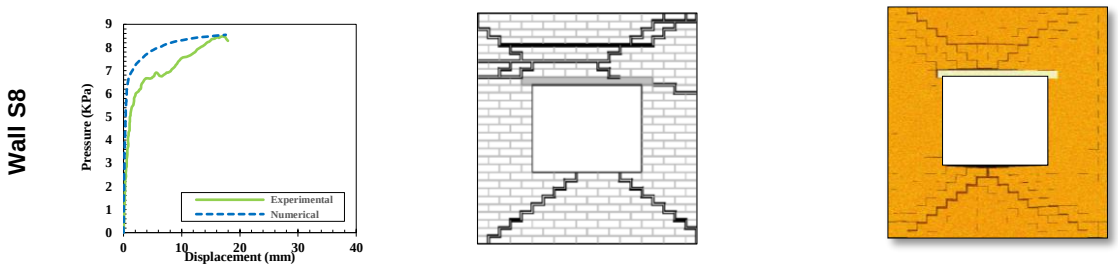

Figure 4. Comparison of experimental and numerical results

5 Conclusions

Applied Element Method was employed to model the OOP behaviour of single-leaf unreinforced masonry walls of typical Australian URM buildings. Results showed that AEM predicted both the pressure-displacement curve and crack pattern very close to the experimental results. However, the method overpredicted the initial wall stiffness. This study is being continued further by verifying modelling technique for dynamic loading and using it to assess the seismic fragility of Queensland's URM building prototypes.

6 Acknowledgement

This research was conducted with the financial support provided by the Australian Government through Australian Research Council's Discover Early Career Project (DE180101593). Authors would like to acknowledge the technical support staff from Applied Science International LLC (ASI) for their help and support with using Extreme Loading for Structures software.

7 References

Adhikari, R. and D'Ayala, D., 2019, June. Applied element modelling and pushover analysis of unreinforced masonry buildings with flexible roof diaphragm. In *7th International Conference on Computational Methods in Structural Dynamics and Earthquake Engineering*. European Community on Computational Methods in Applied Sciences (ECCOMAS).

ASI (2020). Extreme Loading for Structures v8. Applied Science International LLC, Durham (NC), USA.

Asteris, P. G., Sarhosis, V., Mohebkhah, A., Plevris, V., Papaloizou, L., Komodromos, P., and Lemos, J. V. (2015). Numerical modeling of historic masonry structures. In Handbook of research on seismic assessment and rehabilitation of historic structures (pp. 213-256). IGI Global.

Calò, M., Malomo, D., Gabbianelli, G., & Pinho, R. (2021). Shake-table response simulation of a URM building specimen using discrete micro-models with varying degrees of detail. Bulletin of Earthquake Engineering, pp 1-24.

D'Altri, A. M., Sarhosis, V., Milani, G., Rots, J., Cattari, S., Lagomarsino, S., S. Elio, T. Antonio, C. Giovanni and de Miranda, S. (2019). Modeling strategies for the computational analysis of unreinforced masonry structures: review and classification, Archives of Computational Methods in Engineering, Vol 27, No 4, pp 1153-1185.

Galvez, F., Ip, K., Vaculik, J., Griffith, M., Sorrentino, L., Dizhur, D. and Ingham, J.M., 2017, November. Discrete Element Modelling to Predict Failure Strength of Unreinforced

Masonry Walls. In *Proceedings of the Australian Earthquake Engineering Society 2017 Conference*. Nov 24-26, Canberra, ACT.

Galvez, F., Segatta, S., Giaretton, M., Walsh, K., Giongo, I. and Dizhur, D., 2018, June. FE and DE modelling of out-of-plane two way bending behaviour of unreinforced masonry walls. In *16th European Conference on Earthquake Engineering. Thessaloniki, Greece*.

Griffith, M.C. and Vaculik, J., (2007). Out-of-plane flexural strength of unreinforced clay brick masonry walls. TMS Journal, Vol 25, No 1, pp 53-68.

Grunwald, C., Khalil, A. A., Schaufelberger, B., Ricciardi, E. M., Pellecchia, C., De Iuliis, E., & Riedel, W. (2018). Reliability of collapse simulation–Comparing finite and applied element method at different levels. Engineering Structures, Vol 176, pp 265-278.

Jough, F.K.G. and Golhashem, M., (2020). Assessment of out-of-plane behavior of non-structural masonry walls using FE simulations. Bulletin of Earthquake Engineering, Vol 18, No 14, pp 6405-6427.

Malomo, D., Comini, P., Pinho, R. and Penna, A., 2018a. The applied element method and the modelling of both in-plane and out-of-plane response of URM walls. *In the Proceedings of the 16th European Conference on Earthquake Engineering, 16ECEE*, 18-21 June, Thessaloniki, Greece.

Malomo, D., Morandini, C., Crowley, H., Pinho, R. and Penna, A., (2021). Impact of ground floor openings percentage on the dynamic response of typical Dutch URM cavity wall structures. Bulletin of Earthquake Engineering, Vol 19, No 1, pp 403-428.

Malomo, D., Pinho, R., and Penna, A. (2018b). Using the applied element method for modelling calcium silicate brick masonry subjected to in-plane cyclic loading. Earthquake Engineering & Structural Dynamics, Vol 47, No 7, pp 1610-1630.

Malomo, D., Pinho, R., and Penna, A. (2020a). Applied element modelling of the dynamic response of a full-scale clay brick masonry building specimen with flexible diaphragms. International Journal of Architectural Heritage, Vol 14, No 10, pp 1484-1501.

Malomo, D., Pinho, R., and Penna, A. (2020b). Simulating the shake table response of unreinforced masonry cavity wall structures tested to collapse or near-collapse conditions. Earthquake Spectra, Vol 36, No 2, pp 554-578.

Malomo, D., Pinho, R., and Penna, A. (2020c). Numerical modelling of the out-of-plane response of full-scale brick masonry prototypes subjected to incremental dynamic shake-table tests. Engineering Structures, Vol 209, pp 110298.

Meguro, K., and Tagel-Din, H. (1997). A new efficient technique for fracture analysis of structures. Bulletin of Earthquake Resistant Structure Research Center, Vol 30, pp 103-116.

Noor-E-Khuda, S., Dhanasekar, M., and Thambiratnam, D. P. (2016). An explicit finite element modelling method for masonry walls under out-of-plane loading. Engineering Structures, Vol 113, pp 103-120.

Vaculik J. (2012). Unreinforced masonry walls subjected to out-of-plane seismic actions, Ph.D Thesis, Faculty of Civil Engineering, University of Adelaide, Australia.

Yu, S., C. Wu, and M. C. Griffith. 2008. Numerical analysis of out-of-plane loaded masonry wall using homogenization technique. *In The 14th international brick and block masonry conference in Sydney*, pp. 17-20.